Available online at www.sciencedirect.com

ScienceDirect

*Mendeleev Commun.*, 2021, **31**, 721–722

Mendeleev Communications

# Casting synthesis of $Bi_{12}SiO_{20}$

**Timofey V. Bermeshev,*[a] Vladimir P. Zhereb,[a,b] Andrey S. Yasinskiy,[a,c] Elena V. Mazurova,[d] Mikhail P. Bundin,[a] Alexander S. Samoilo,[a] Vadim M. Bespalov,[a] Nadezhda V. Merdak,[a] Olga V. Yushkova,[a] Pavel O. Yuryev[a] and Alexander I. Bezrukikh[a]**

[a] *Siberian Federal University, 660041 Krasnoyarsk, Russian Federation. E-mail: irbis_btv@mail.ru*
[b] *M. F. Reshetnev Siberian State University of Science and Technology, 660037 Krasnoyarsk, Russian Federation*
[c] *Institute of Process Metallurgy and Metal Recycling, RWTH Aachen University, 52056 Aachen, Germany*
[d] *Institute of Chemistry and Chemical Technology, Siberian Branch of the Russian Academy of Sciences, 660036 Krasnoyarsk, Russian Federation*

DOI: 10.1016/j.mencom.2021.09.043

**Polycrystalline bismuth silicate $Bi_{12}SiO_{20}$ has been obtained by fusing a stoichiometric mixture of $Bi_2O_3$ and $SiO_2$ followed by crystallization of the melt by casting with no seeding.**

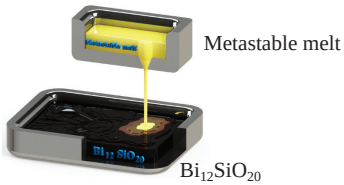


*Keywords*: casting, stable phase, bismuth silicate, melt crystallization, heat treatment.

Bismuth silicate $Bi_{12}SiO_{20}$ with crystalline sillenite structure (CSS) find various applications due to its piezoelectric, photorefractive, photoconductive, magneto-optical and electro-optical properties. Since the 1970s, it has been used in devices for optical information processing,[1–3] piezoelectric sensors, filters and delay lines of electromagnetic signals, electro- and magneto-optical field strength meters, space–time modulators,[4,5] miniature and passive microwave ceramic components with high performance for mobile devices,[6] fiber optic sensors for electric current[7] as well as a filler for materials employed in protection against cosmic rays.[8]

In the $Bi_2O_3$–$SiO_2$ system in stable equilibrium, two bismuth silicates exist, namely congruently melting $Bi_{12}SiO_{20}$ with CSS and incongruently melting $Bi_4Si_3O_{12}$ with the crystal structure of eulythine. In metastable equilibrium of this system, a solid solution is formed from a high temperature modification of δ-$Bi_2O_3$ and bismuth silicate $Bi_2SiO_5$ having a layered crystal of the Aurivillius type. This metastable equilibrium results from crystallization of a supercooled melt in the absence of stable phase seeding, which significantly limits the employment of melting techniques for the synthesis of stable phases as well as the possibility of obtaining optically perfect single crystals with CSS.

It is known,[9] that the $Bi_2O_3$–$SiO_2$ phase diagram in stable equilibrium contains three distinct temperature zones in the region of liquid state marked as A, B and C in Figure S1 (see Online Supplementary Materials), where the state of the melt differs, in addition to its pattern of property–temperature dependences, as well in the phase composition of crystals formed in the crystallization of slowly cooled melts starting from the temperature values of the zones. To date, the conditions have been determined for the implementation of the stable and metastable equilibrium states at slow cooling of the melt, namely 5–10 °C $min^{-1}$.[10–12] Metastable equilibria, in contrast to the stable equilibrium, can be described by more than one phase diagram. The metastable equilibria, which appear in the $Bi_2O_3$–$SiO_2$ system upon slow cooling of the melt starting from temperature values of zones B and C (see Figure S1), differ mainly in the character of crystallization and the occurrence of the melt delamination.[13]

Single crystals of $Bi_{12}SiO_{20}$ are typically grown from a melt obtained in turn by heating a charge of $Bi_{12}SiO_{20}$. To prevent contamination of the charge with metastable phases, the preliminary synthesis of $Bi_{12}SiO_{20}$ can be carried out by chemical[14] and solid-phase[15] methods, mechanical alloying,[16] molten salt method[17] as well as hydrothermal[18] or combined[19] technique. However, the melt method seems to be the superior one in terms of economic indicators and manufacturability. Therefore, the investigation of melts crystallization under various conditions is of both fundamental and practical interest. In our work[20] it has been demonstrated that using thermal treatment of the melt it is possible to control the processes of phase formation in bismuth oxide-containing systems.

The aim of this work was to investigate the conditions for obtaining a compound with CSS during the crystallization of a stoichiometric melt. The synthesis of $Bi_{12}SiO_{20}$ was carried out in a Pt crucible,† then the melt was poured onto a Pt plate. The samples obtained were investigated using the methods of macro- and microstructural analysis as well as powder X-ray diffraction (XRD).‡

† For the preparation of initial samples of 10 g weight each, equimolar amounts of α-$Bi_2O_3$ and amorphous $SiO_2$, both of the puriss. grade, were mixed, placed in 32 $cm^3$ Pt crucibles, heated in an LMV 02/12 electric furnace (LAC, Czech Republic) under air up to a temperature corresponding to zone C (see Figure S1), namely 1100 °C, at a rate of ~20 °C $min^{-1}$, and kept under isothermal conditions for 1 h. Then the melts were poured from the crucibles onto a Pt plate at room temperature.

‡ The surface macrostructure of the samples was examined using a Stemi 2000 stereoscope (Carl Zeiss). The microstructure was investigated on an Axio Observer.A1 optical microscope (Carl Zeiss) using microslices obtained after grinding, polishing and etching. X-ray powder diffraction data were collected on a Shimadzu XRD 6000 diffractometer using CuKα radiation.

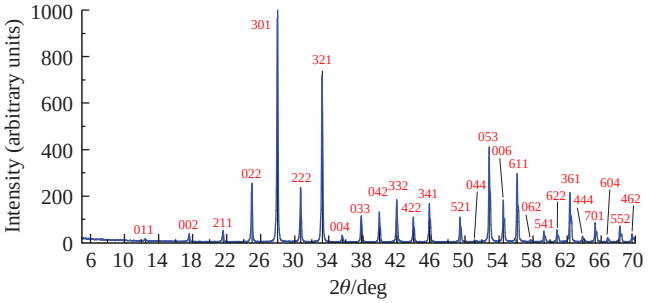


**Figure 1** XRD pattern of sample obtained by crystallization of the melt from the temperature zone C by casting onto Pt substrate.

According to the XRD results, a sample obtained by pouring a melt from the temperature zone C onto Pt substrate at room temperature represents single-phase bismuth silicate $Bi_{12}SiO_{20}$ having CSS (Figure 1). This diffraction pattern was found in the ICDD PDF2 database as card no. 00-037-0485, the crystal structure being similar to the one of compound no. 1533225 in the Crystallography Open Database.[21] Average domain size calculated by the Scherrer formula is 192 μm. Note, that this analysis is a semi-quantitative one and impurity phases up to 1–2 wt% typically are not visible in the diffractogram.

The macrostructure of the dark grey colored cast sample at its base represents columnar crystals grown in the direction of the heat removal. The upper part of the sample, where the melt has continued to flow to the crystallized part, consists of a group of massive pyramid-shaped crystals [Figure 2(*a*)]. The texture of the material in contact with the Pt substrate represents an array of oriented small crystals [Figure 2(*b*)].

Samples obtained by casting from the temperature zone C have homogeneous microstructure. At the interface between the sample and the Pt substrate, where the cooling rate has been the highest, the grains have a characteristic dendrite shape and small size [Figure 3(*a*)]. This layer has low thickness, and the main part of the sample, which has not been in direct contact with the cold substrate, consists of massive grains elongated in the direction of heat removal [Figure 3(*b*)]. The sample also contains pores and cracks due to thermal stress at the sharp temperature drop.

Thus, bismuth silicate $Bi_{12}SiO_{20}$ with CSS was obtained after melting stoichiometric mixture of initial oxides in a Pt crucible, isothermal holding at a temperature of zone C (see Figure S1) and the following pouring the melt onto Pt substrate at room temperature, *i.e.*, by the casting method. Metastable phases in the $Bi_2O_3$–$SiO_2$ system are formed due to transition of the melt to a metastable state after its heat treatment, which apparently retains the structure of a high temperature melt with the polymerization of its structural components and the microheterogeneity, which is subsequently transformed into macro-delamination. Monotonic cooling of metastable melt from temperatures of zone C without thermal gradients, vibration or shock effects contributes to the preservation of the polymer structure, overcooling and crystallization of metastable phases. The melt casting approach creates extremely high temperature gradients in the melt, ensuring the transition of the system to the stable equilibrium state. Pouring the melt onto Pt substrate in the casting method represents a thermal shock that initiates the formation and growth of the stable phase nuclei.

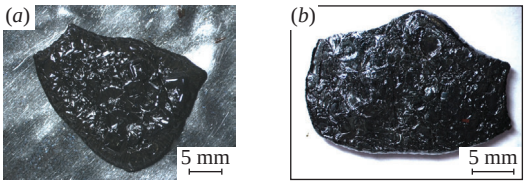


**Figure 2** Macrostructure of sample obtained by casting onto Pt substrate from the temperature zone C: (*a*) 1.25× top view, (*b*) 1.6× bottom view of the side in contact with the Pt plate.

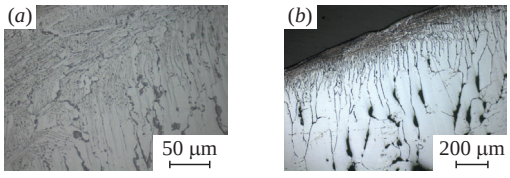


**Figure 3** Microstructure of sample obtained by casting onto Pt substrate upon cooling from the temperature zone C with magnification (*a*) 500× and (*b*) 100×.

This work is carried out as a part of the State Assignment for the Science of Siberian Federal University (project no. FSRZ-2020-0013). The use of equipment of the Krasnoyarsk Regional Center of Research Equipment of the Federal Research Center 'Krasnoyarsk Science Center, SB RAS' is gratefully acknowledged.

*Online Supplementary Materials*

Supplementary data associated with this article can be found in the online version at doi: 10.1016/j.mencom.2021.09.043.

## References

1 P. Vohl, P. Nisenson and D. S. Oliver, *IEEE Trans. Electron Devices*, 1973, **20**, 1032.
2 J. O. White and A. Yariv, *Appl. Phys. Lett.*, 1980, **37**, 5.
3 E. Burattini, G. Cappuccio, M. C. Ferrari, M. Grandolfo, P. Vecchia and Sh. M. Efendiev, *J. Opt. Soc. Am. B*, 1988, **5**, 714.
4 V. N. Shlegel and D. S. Pantsurkin, *Crystallogr. Rep.*, 2011, **56**, 339 (*Kristallografiya*, 2011, **56**, 367).
5 M. Mori, Y. Yagai, T. Yatagai and M. Watanabe, *Appl. Opt.*, 1998, **37**, 2852.
6 B.-J. Jeong, M.-R. Joung, S.-H. Kweon, J.-S. Kim, S. Nahm, J.-W. Choi and S.-J. Hwang, *Mater. Res. Bull.*, 2012, **47**, 4510.
7 A. N. Demin, V. I. Smyslov and A. T. Klement'ev, *Izmerenie. Monitoring. Upravleniye. Kontrol'*, 2016, **2** (16), 28 (in Russian).
8 A. V. Pavlenko, N. I. Cherkashina, R. N. Yastrebinsky and A. V. Noskov, *Vopr. At. Nauki Tekh., Ser.: Yad.-Fiz. Issled.*, 2017, no. 5, 21 (in Russian).
9 Yu. F. Kargin, V. P. Zhereb and V. M. Skorikov, *Russ. J. Inorg. Chem.*, 1991, **36**, 1466 (*Zh. Neorg. Khim.*, 1991, **36**, 2611).
10 I. V. Tananaev, V. M. Skorikov, Yu. F. Kargin and V. P. Zhereb, *Izv. Akad. Nauk SSSR, Neorg. Mater.*, 1978, **14**, 2024 (in Russian).
11 V. P. Zhereb, Yu. F. Kargin and V. M. Skorikov, *Izv. Akad. Nauk SSSR, Neorg. Mater.*, 1978, **14**, 2029 (in Russian).
12 V. P. Zhereb and V. M. Skorikov, *Inorg. Mater.*, 2003, **39**, S121.
13 V. P. Zhereb, *PhD Thesis*, Institute of General and Inorganic Chemistry, USSR Academy of Sciences, Moscow, 1980.
14 H. Zhang, Y. Feng, S. Jia, D. Jiang and Q. Zhan, *Appl. Surf. Sci.*, 2020, **520**, 146355.
15 B.-J. Jeong, M.-R. Joung, S.-H. Kweon, J.-S. Kim, S. Nahm, J.-W. Choi and S.-J. Hwang, *J. Am. Ceram. Soc.*, 2013, **96**, 2225.
16 I. F. Vasconcelos, M. A. Pimenta and A. S. B. Sombra, *J. Mater. Sci.*, 2001, **36**, 587.
17 J. Lu, X. Wang and H. Jiang, *Appl. Mech. Mater.*, 2012, **182–183**, 52.
18 A. A. Vodyankin, I. P. Ushakov, Yu. A. Belik and O. V. Vodyankina, *Kinet. Catal.*, 2017, **58**, 593 (*Kinet. Katal.*, 2017, **58**, 606).
19 S. Fu and H. Ozoe, *J. Phys. D: Appl. Phys.*, 1996, **29**, 2032.
20 V. P. Zhereb, T. V. Bermeshev, Yu. F. Kargin, E. V. Mazurova and V. M. Denisov, *Inorg. Mater.*, 2019, **55**, 737 (*Neorg. Mater.*, 2019, **55**, 782).
21 S. Gražulis, A. Daškevič, A. Merkys, D. Chateigner, L. Lutterotti, M. Quirós, N. R. Serebryanaya, P. Moeck, R. T. Downs and A. Le Bail, *Nucleic Acids Res.*, 2012, **40**, D420.

*Received: 12th April 2021; Com. 21/6519*